Available online at www.sciencedirect.com
SCIENCE DIRECT®
Journal of Sound and Vibration 275 (2004) 27–45
JOURNAL OF SOUND AND VIBRATION
www.elsevier.com/locate/jsvi

Interaction of Hopf and period doubling bifurcations of a vibro-impact system

W.-C. Ding[a,*], J.H. Xie[b], Q.G. Sun[a]

[a] School of Mechanical Engineering, Lanzhou Jiaotong University, Lanzhou 730070, People's Republic of China
[b] Department of Applied Mechanics and Engineering, Southwest Jiaotong University, Chengdu 610031, People's Republic of China

Received 16 April 2003; accepted 24 June 2003

Abstract

An inertial shaker as a vibratory system with impact is considered. By means of differential equations, periodicity and matching conditions, the theoretical solution of periodic $n-1$ impacting motion can be obtained and the Poincaré map is established. Dynamics of the system are studied with special attention to interaction of Hopf and period doubling bifurcations corresponding to a codimension-2 one when a pair of complex conjugate eigenvalues crosses the unit circle and the other eigenvalue crosses -1 simultaneously for the Jacobi matrix. The four-dimensional map can be reduced to a three-dimensional normal form by the center manifold theorem and the theory of normal forms. The two-parameter unfoldings of local dynamical behavior are put forward and the singularity is investigated. It is proved that there exist curve doubling bifurcation (a torus doubling bifurcation), Hopf bifurcation of 2–2 fixed points as well as period doubling bifurcation and Hopf bifurcation of 1–1 fixed points near the critical point. Numerical results indicate that the vibro-impact system presents complicated and interesting curve doubling bifurcation and Hopf bifurcation as the two controlling parameters vary.

1. Introduction

Vibro-impact systems are often encountered in practice, for instance, in the models of hammer-like devices, rotor-casing dynamical systems, collisions of solids, ships moored at dockside, etc. Impacts give rise to non-linearity and discontinuity so that the vibro-impact system can exhibit rich and complicated dynamic behavior and it is a good testing bench for non-linear theories [1–10]. During the past decades non-smooth dynamics of mechanical systems with impacts have

*Corresponding author.
E-mail address: dingdd@163.com (W.-C. Ding).

0022-460X/$ - see front matter © 2003 Elsevier Ltd. All rights reserved.
doi:10.1016/S0022-460X(03)00740-5

become the subject of several investigations, and many new problems of theory have been advanced in research of vibro-impacts. The classical pattern of period doubling bifurcation cascade was observed numerically by Shaw and Holmes [1]. Nordmark [2] proved that such systems can undergo "grazing bifurcation" and that they could lead to chaotic behavior. Peterka and Vacik [3] even provided bounds of chaotic responses with the help of an analogue computer. Recently, a few researchers began to focus their attention on the phenomena of Hopf bifurcations of the vibro-impact systems. Chatterjee and Mallik [4] studied quasi-periodic vibro-impacts of a class of single-degree-of-freedom (d.o.f.) self-excited oscillators with an impact damper. Budd [5] studied vibro-impacts of a single-d.o.f. system contacting a single stop and proved that if coefficient of restitution is less than 1, then quasi-periodic motion cannot occur in the system. Luo and Xie [6–8] considered a 2-d.o.f. vibro-impact system without damping, and studied Hopf bifurcations of periodic motions with single impact in non-resonance, weak resonance and strong resonance cases. So far, few researchers have investigated the phenomena of codimension-2 bifurcation in vibro-impact system. Xie [9] and Wen [10] investigated codimension-2 bifurcations corresponding to eigenvalues being double -1 of a vibro-impact system with one-side amplitude constraint and found Hopf bifurcation of period 2 two-impact orbit.

In this paper, using Poincaré map and normal form approach, we investigate the interaction of Hopf and period doubling bifurcation (the so-called Hopf–Flip bifurcation [11]) of inertial impacting shaker, which is a 2-d.o.f. vibro-impact system. To make it possible to analyze this complex problem and make the calculations easier and correct, we take advantage of a symbolic software, like MAPLE. In the second section of this paper, the equations of motion are discussed and the Poincaré map is established, then periodic motion with one impact and its stability are studied by analytical methods. The normal forms in Hopf-zero cases for differential equations are discussed in Ref. [12]. In Section 3, we propose the procedure to reduce the four-dimensional maps to a three-dimensional ones by the center manifold theorem and determine the normal forms and the associated coefficients, and we discuss Hopf–Flip bifurcations of the vibro-impact system, which correspond to a codimension-2 situation when a pair of complex conjugate eigenvalues crosses the unit circle and the other eigenvalue crosses -1 simultaneously for the Jacobi matrix. In Section 4, numerical simulation proves that there exist curve doubling bifurcation (a torus doubling bifurcation), Hopf bifurcation of 2–2 fixed points as well as period doubling bifurcation and Hopf bifurcation of 1–1 fixed points near the critical point.

2. Poincare map, periodic motions and its stability

The model for one type of 2-d.o.f. vibro-impact system is shown in Fig. 1. The mass M is connected to a linear spring with stiffness K and a damper C. The excitation on M is harmonic with amplitude F_0. The mass M will impact mass m whenever they have the same height and a non-zero relative velocity. After impacting, m becomes a free body and moves in the field of gravity g, while M becomes a 1-d.o.f. forced oscillator. The situation lasts till the next impact.

Between impacts, the governing equations are

$$M\ddot{x} + C\dot{x} + Kx = F_0 \sin(\omega t + \delta), \tag{1}$$

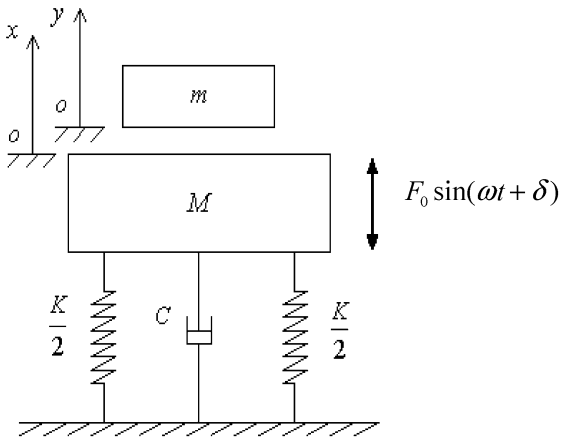

Fig. 1. Schematic of the vibro-impact system.

$$\ddot{y} = -g. \tag{2}$$

According to the conservation law of momentum and the definition of coefficient of restitution R, we have

$$M\dot{x}_- + m\dot{y}_- = M\dot{x}_+ + m\dot{y}_+, \tag{3}$$

$$\dot{x}_+ - \dot{y}_+ = -R(\dot{x}_- - \dot{y}_-), \tag{4}$$

where $\dot{x}_-$ and $\dot{y}_-$ represent, respectively, the approach velocities of M and m at the instant of impact. $\dot{x}_+$ and $\dot{y}_+$ represent, respectively, the departure velocities of M and m at the instant, which are given by

$$\dot{x}_+ = \frac{1-\mu R}{1+\mu}\dot{x}_- + \frac{\mu(1+R)}{1+\mu}\dot{y}_-, \quad \dot{y}_+ = \frac{1+R}{1+\mu}\dot{x}_- + \frac{\mu - R}{1+\mu}\dot{y}_-, \tag{5}$$

where $\mu = m/M$.

We use new scaling $x = A\bar{x}$, $y = A\bar{y}$, $\theta = \omega t$, where $A = F_0/(K\sqrt{(1-\gamma^2)^2 + (2\xi\gamma)^2})$, and drop the bar for convenience. We put Eqs. (1) and (2) (as well as Eq. (5)) into non-dimensional forms

$$\ddot{x} + \frac{2\xi}{\gamma}\dot{x} + \frac{1}{\gamma^2}x = \frac{\sqrt{(1-\gamma^2)^2 + (2\xi\gamma)^2}}{\gamma^2}\sin(\theta + \delta), \tag{6}$$

$$\ddot{y} = -e_1, \tag{7}$$

where $\gamma = \omega/\omega_n$, $\omega_n = \sqrt{K/M}$, $\xi = C/(2M\omega_n)$, $e_1 = \sqrt{(1-\gamma^2)^2 + (2\xi\gamma)^2}/(\beta\gamma^2)$, $\beta = F_0/Mg$.

The full solutions of Eqs. (6) and (7) take the forms

$$x(\theta) = \mathrm{e}^{-\xi(\theta/z)}[b_1 \sin\eta(\theta/\gamma) + b_2 \cos\eta(\theta/\gamma)] + \sin(\theta + \tau), \tag{8}$$

$$\begin{aligned}\dot{x}(\theta) = {} & [\mathrm{e}^{-\xi(\theta/z)}/\gamma]\{[b_1[\eta\cos\eta(\theta/\gamma) - \xi\sin\eta(\theta/\gamma)] \\ & - b_2[\xi\cos\eta(\theta/\gamma) + \eta\sin\eta(\theta/\gamma)]\} + \cos(\theta + \tau),\end{aligned} \tag{9}$$

$$y(\theta) = b_3 + b_4\theta - e_1\theta^2/2, \tag{10}$$

$$\dot{y}(\theta) = b_4 - e_1\theta, \tag{11}$$

where $\eta = \sqrt{1-\xi^2}$, $\tau = \delta - \varphi$, $\varphi = \tan^{-1}[2\xi\gamma/(1-\gamma^2)]$ and b_i $(i = 1, \ldots, 4)$ are constants.

We choose a Poincaré section: $\sigma \subset \mathbf{R}^4 \times \mathbf{S}^1$, where $\sigma = \{(x, \dot{x}, y, \dot{y}, \theta) \in \mathbf{R}^4 \times \mathbf{S}^1, x = y, \dot{x} = \dot{x}_+, \dot{y} = \dot{y}_+\}$, $\mathbf{S}^1 = \mathbf{R} \pmod{T}$ reflects the periodicity of period T in t. Suppose the nth impact occurs at $\theta = 0^+$, the state variables of the system at $\theta = 0^+$ is $(\tilde{x}, \dot{\tilde{x}}, \tilde{x}, \dot{\tilde{y}})^{\mathrm{T}}$, and b_i $(i = 1, \ldots, 4)$ can be easily represented by the state variables and phase $\tilde{\tau}$. So, we have

$$x(\theta) = x(\theta, \tilde{x}, \dot{\tilde{x}}, \tilde{\tau}), \tag{12}$$

$$\dot{x}(\theta) = \dot{x}(\theta, \tilde{x}, \dot{\tilde{x}}, \tilde{\tau}), \tag{13}$$

$$y(\theta) = y(\theta, \tilde{x}, \dot{\tilde{y}}), \tag{14}$$

$$\dot{y}(\theta) = \dot{y}(\theta, \dot{\tilde{y}}). \tag{15}$$

Suppose θ is the smallest positive root of the equation

$$G(\theta, \tilde{x}, \dot{\tilde{x}}, \dot{\tilde{y}}, \tilde{\tau}) = x(\theta, \tilde{x}, \dot{\tilde{x}}, \tilde{\tau}) - y(\theta, \tilde{x}, \dot{\tilde{y}}) = 0, \tag{16}$$

then at the instant θ, the $(n+1)$th impact happens. From Eq. (5) and the continuity of displacement of M during the impact, we obtain the state variables at $\theta = \theta^+$

$$x' = x(\theta^+, \tilde{x}, \dot{\tilde{x}}, \tilde{\tau}) = x(\theta, \tilde{x}, \dot{\tilde{x}}, \tilde{\tau}) = \hat{f}_1(\theta, \tilde{x}, \dot{\tilde{x}}, \tilde{\tau}), \tag{17}$$

$$\begin{aligned} \dot{x}' &= \dot{x}(\theta^+, \tilde{x}, \dot{\tilde{x}}, \dot{\tilde{y}}, \tilde{\tau}) = \hat{f}_2(\theta, \tilde{x}, \dot{\tilde{x}}, \dot{\tilde{y}}, \tilde{\tau}) \\ &= \frac{1-\mu R}{1+\mu}\dot{x}(\theta^-, \tilde{x}, \dot{\tilde{x}}, \tilde{\tau}) + \frac{\mu(1+R)}{1+\mu}\dot{y}(\theta^-, \dot{\tilde{y}}), \end{aligned} \tag{18}$$

$$\begin{aligned} \dot{y}' &= \dot{y}(\theta^+, \tilde{x}, \dot{\tilde{x}}, \dot{\tilde{y}}, \tilde{\tau}) = \hat{f}_3(\theta, \tilde{x}, \dot{\tilde{x}}, \dot{\tilde{y}}, \tilde{\tau}) \\ &= \frac{1+R}{1+\mu}\dot{x}(\theta^-, \tilde{x}, \dot{\tilde{x}}, \tilde{\tau}) + \frac{\mu-R}{1+\mu}\dot{y}(\theta^-, \dot{\tilde{y}}). \end{aligned} \tag{19}$$

The following relationship is obvious:

$$\tau' = \theta + \tilde{\tau} (\mathrm{mod}\, 2\pi). \tag{20}$$

If there is a point $(\theta, \tilde{x}, \dot{\tilde{x}}, \dot{\tilde{y}}, \tilde{\tau})^{\mathrm{T}} \in \mathbf{S}^1 \times \mathbf{R}^3 \times \mathbf{S}^1$, which satisfies Eq. (16) and

$$G'_\theta(\theta, \tilde{x}, \dot{\tilde{x}}, \dot{\tilde{y}}, \tilde{\tau}) = \dot{x}(\theta, \tilde{x}, \dot{\tilde{x}}, \tilde{\tau}) - \dot{y}(\theta, \tilde{x}, \dot{\tilde{y}}) \neq 0 \tag{21}$$

at the same point. By virtue of the implicit function theorem, θ can locally be solved from Eq. (16) as

$$\theta = \theta(\tilde{x}, \dot{\tilde{x}}, \dot{\tilde{y}}, \tilde{\tau}). \tag{22}$$

Inserting Eq. (22) into Eqs. (17)–(20), without loss of generality, $(\tilde{x}, \dot{\tilde{x}}, \dot{\tilde{y}}, \tilde{\tau})$ is still represented by $(x, \dot{x}, \dot{y}, \tau)$ and we obtain the Poincaré map

$$f : \Omega \to \mathbf{R}^3 \times \mathbf{S}^1 \tag{23}$$

or

$$\begin{aligned} x' &= f_1(x, \dot{x}, \dot{y}, \tau) = \hat{f}_1(\theta(x, \dot{x}, \dot{y}, \tau), x, \dot{x}, \tau), \\ \dot{x}' &= f_2(x, \dot{x}, \dot{y}, \tau) = \hat{f}_2(\theta(x, \dot{x}, \dot{y}, \tau), x, \dot{x}, \dot{y}, \tau), \\ \dot{y}' &= f_3(x, \dot{x}, \dot{y}, \tau) = \hat{f}_3(\theta(x, \dot{x}, \dot{y}, \tau), x, \dot{x}, \dot{y}, \tau), \\ \tau' &= f_4(x, \dot{x}, \dot{y}, \tau) = \theta(x, \dot{x}, \dot{y}, \tau) + \tau (\mathrm{mod}\, 2\pi), \end{aligned} \tag{24}$$

where $\Omega \subset \mathbf{R}^3 \times \mathbf{S}^1$ is a connected open domain. If there exists a point

$$(2n\pi, x_0, \dot{x}_0, \dot{y}_0, \tau_0)^{\mathrm{T}} \in \mathbf{S}^1 \times \mathbf{R}^3 \times \mathbf{S}^1,$$

which satisfies Eqs. (16), (21) and

$$\begin{aligned} x_0 &= \hat{f}_1(2n\pi, x_0, \dot{x}_0, \tau_0), \\ \dot{x}_0 &= \hat{f}_2(2n\pi, x_0, \dot{x}_0, \dot{y}_0, \tau_0), \\ \dot{y}_0 &= \hat{f}_3(2n\pi, x_0, \dot{x}_0, \dot{y}_0, \tau_0). \end{aligned} \tag{25}$$

then $X_0 = (x_0, \dot{x}_0, \dot{y}_0, \tau_0)^{\mathrm{T}} \in \mathbf{R}^3 \times \mathbf{S}^1$ is a fixed point of map (23), or $f(X_0) = X_0$.

Replacing $\tilde{x}, \dot{\tilde{x}}, \dot{\tilde{y}}, \tilde{\tau}$ in Eqs. (12)–(15), respectively, by $x_0, \dot{x}_0, \dot{y}_0, \tau_0$, we obtain a period nT motion of the system, which is periodic $n-1$ impact motion, where $T = 2n\pi/\omega$.

Due to the weak dynamical coupling nature of the system, the period nT motion can easily be computed from Eqs. (16) and (25) and be represented as functions of parameters (in the case $n = 1$, see Appendix A). The stability of the period nT motion is equivalent to that of the fixed point X_0 of map (23), the latter is determined by the matrix

$$Df(X_0) = \left.\frac{\partial f(X)}{\partial X}\right|_{X=X_0}, \tag{26}$$

where $X = (x, \dot{x}, \dot{y}, \tau)^{\mathrm{T}} \in \mathbf{R}^3 \times \mathbf{S}^1$. If all eigenvalues of $Df(X_0)$ lie inside of the unit circle, the fixed point is stable, so is the period nT motion. If some eigenvalues that pass the boundary of the unit circle, the fixed point X_0 loses its stability, and so does the period nT motion. In this case, bifurcation may happen. The type of the bifurcation depends not only on the degeneracy of $Df(X_0)$ but also on high terms in f.

All entries of $Df(X_0)$ can be computed and are represented as functions of system parameters. For example

$$\frac{\partial f_1}{\partial x} = \frac{\partial \hat{f}_1}{\partial \theta}\frac{\partial \theta}{\partial x} + \frac{\partial \hat{f}_1}{\partial x}, \quad \left(\frac{\partial \theta}{\partial x} = -\frac{\partial G/\partial x}{\partial G/\partial \theta}\right). \tag{27}$$

$Df(X_0)$ is given in Appendix B.

Let $\Delta X = X - X_0$, we change Eq. (23) into

$$f_v : \Omega \to \mathbf{R}^4,$$

$$\Delta X' = f_v(\Delta X) = f(X_0(v) + \Delta X) - X_0(v), \tag{28}$$

where Ω stands for a connected open domain containing the origin of $\mathbf{R}^4$, and $v = (v_1, v_2)^{\mathrm{T}} \in \mathbf{R}^2$ represents parameter set of the system.

We expand the function$f_v(\Delta X)$ as Taylor series in the variables ΔX and v, which takes the form

$$f_v(\Delta X) = \sum_{p+q\geqslant 1} F_{pq} v^p \Delta X^q \tag{29}$$

with

$$F_{pq} = \frac{1}{p!q!} \frac{\partial^{p+q} f_v(\Delta X)}{\partial v^p \partial \Delta X^q}\bigg|_{(v_c,0)}, \quad F_{P0} \equiv 0, \quad p \geqslant 1, \tag{30}$$

where v_c is a critical parameter value.

3. Interaction of Hopf and period doubling bifurcation

We will reduce the four-dimensional maps (28) to a three-dimensional normal form by the center manifold theorem and theory of normal forms in this section. The Jacobian matrix of Eq. (28) at $\Delta X = 0$ reads

$$A(v) = Df_v(0). \tag{31}$$

Take $\bar{v} = v - v_c$, and drop the bar for convenience. We study one kind of codimension-2 bifurcation of system (1), which is characterized by the so-called Hopf–Flip degeneracy, and satisfy:

(H.1) $A(0) = Df_0(0)$ has a pair of complex conjugate eigenvalues $\lambda_0, \overline{\lambda_0}$ on the unit circle, one real eigenvalues $\lambda_1 = -1$, and another real eigenvalue $|\lambda_2| < 1$.

(H.2) Non-resonant condition $\lambda_0^n \neq 1$, $n = 1, 2, 3, 4, 5, 6$ and $\lambda_0^n \neq -1$, $n = 4, 5$.

Let

$$p(\lambda) = \lambda^4 + a_3\lambda^3 + a_2\lambda^2 + a_1\lambda + a_0 = 0 \tag{32}$$

be characteristic equation for matrix $A(v)$, then we have the following useful lemma [13]:

Lemma. *The roots of Eq.* (32) *satisfy* (H.1), *if and only if*

(a.1) $|a_0| < 1$;
(a.2) $a_1 + a_3 = 1 + a_0 + a_2$;
(a.3) $a_2(1 - a_0) + a_0(1 - a_0^2) + a_3(a_0a_3 - a_1) = a_0a_2(1 - a_0) + (1 - a_0^2) + a_1(a_0a_3 - a_1) = 0$;
(a.4) $a_1 + a_3 > 0$; *and*
(a.5) $2a_0 + a_3 < 2 + a_1$,

where $a_i \in \mathbf{R}$ $(i = 0, 1, 2, 3, 4, 5)$ *is dependent upon parameters of the system.*

We write four-dimensional map (29) as

$$x' = Ax + F(x) = Ax + F^2(x) + F^3(x) + O(\|x\|^4), \tag{33}$$

where $A = A(0)$, $x = (x_1, x_2, x_3, x_4)^{\mathrm{T}} = (\Delta x, \Delta\dot{x}, \Delta\dot{y}, \Delta\tau)^{\mathrm{T}}$, $F^m = (F^m_{(1)}, F^m_{(2)}, F^m_{(3)}, F^m_{(4)})^{\mathrm{T}}$ and $F^m_{(j)}$ is the jth component of F^m, in which

$$F^2_{(j)} = \sum_{\bar{s}=2} \frac{1}{s_1!s_2!s_3!s_4!} \frac{\partial^{\bar{s}} F_{(j)}}{\partial x_1^{s_1}\partial x_2^{s_2}\partial x_3^{s_3}\partial x_4^{s_4}} x_1^{s_1} x_2^{s_2} x_3^{s_3} x_4^{s_4},$$

$$F^3_{(j)} = \sum_{\bar{s}=3} \frac{1}{s_1!s_2!s_3!s_4!} \frac{\partial^{\bar{s}} F_{(j)}}{\partial x_1^{s_1}\partial x_2^{s_2}\partial x_3^{s_3}\partial x_4^{s_4}} x_1^{s_1} x_2^{s_2} x_3^{s_3} x_4^{s_4},$$

where $j = 1, \ldots, 4$, $\bar{s} = s_1 + s_2 + s_3 + s_4$. Let $q_1 \in \mathbf{R}^4$, $q_2 \in \mathbf{R}^4$ and $q_0 \in \mathbf{C}^4$ be eigenvectors corresponding to λ_1, λ_2 and λ_0, respectively, we can obtain the eigenmatrix

$$B = (q_1, \mathrm{Re}\, q_0, -\mathrm{Im}\, q_0, q_2). \tag{34}$$

After changing the co-ordinates as $x = B(y^{\mathrm{T}}, w)^{\mathrm{T}}$, we put map of Eq. (33) into the form

$$y' = B_0 y + H(y, w), \quad w' = \lambda_2 w + E(y, w), \tag{35}$$

where $w \in \mathbf{R}, y = (y_1, y_2, y_3)^{\mathrm{T}} \in \mathbf{R}^3$, $H(y, w) = (H_1, H_2, H_3)^{\mathrm{T}}$ and

$$B_0 = \begin{bmatrix} -1 & 0 & 0 \\ 0 & \alpha & -\beta \\ 0 & \beta & \alpha \end{bmatrix} \quad (\alpha = \mathrm{Re}\,\lambda_0,\ \beta = \mathrm{Im}\,\lambda_0). \tag{36}$$

Let $u = y_1$, $z = y_2 + \mathrm{i}y_3$, $\bar{z} = y_2 - \mathrm{i}y_3$, map (35) takes the form

$$\begin{aligned} u' = & -u + \tfrac{1}{2}g_{200}u^2 + \tfrac{1}{2}g_{020}z^2 + \tfrac{1}{2}g_{002}\bar{z}^2 + g_{110}uz + g_{101}u\bar{z} + g_{011}z\bar{z} \\ & + G_{100}wu + G_{010}wz + G_{001}w\bar{z} + \tfrac{1}{6}g_{300}u^3 + g_{111}uz\bar{z} + f_1(u, z, \bar{z}, y), \end{aligned} \tag{37a}$$

$$\begin{aligned} z' = & \lambda_0 z + \tfrac{1}{2}h_{200}u^2 + \tfrac{1}{2}h_{020}z^2 + \tfrac{1}{2}h_{002}\bar{z}^2 + h_{110}uz + h_{101}u\bar{z} + h_{011}z\bar{z} \\ & + K_{100}wu + K_{010}wz + K_{001}w\bar{z} + \tfrac{1}{2}h_{210}u^2 z + \tfrac{1}{2}h_{021}z^2\bar{z} + f_2(u, z, \bar{z}, y), \end{aligned} \tag{37b}$$

$$w' = \lambda_2 w + \tfrac{1}{2}e_{200}u^2 + \tfrac{1}{2}e_{020}z^2 + \tfrac{1}{2}e_{002}\bar{z}^2 + e_{110}uz + e_{101}u\bar{z} + e_{011}z\bar{z} + \cdots, \tag{37c}$$

where

$$g_{200} = \frac{\partial^2 H_1}{\partial y_1^2}, \quad g_{020} = \frac{1}{4}\left(\frac{\partial^2 H_1}{\partial y_2^2} - \frac{\partial^2 H_1}{\partial y_3^2} - 2\mathrm{i}\frac{\partial^2 H_1}{\partial y_2 \partial y_3}\right),$$

$$g_{002} = \frac{1}{4}\left(\frac{\partial^2 H_1}{\partial y_2^2} - \frac{\partial^2 H_1}{\partial y_3^2} + 2\mathrm{i}\frac{\partial^2 H_1}{\partial y_2 \partial y_3}\right),$$

$$g_{110} = \frac{1}{2}\left(\frac{\partial^2 H_1}{\partial y_1 \partial y_2} - \mathrm{i}\frac{\partial^2 H_1}{\partial y_1 \partial y_3}\right), \quad g_{101} = \frac{1}{2}\left(\frac{\partial^2 H_1}{\partial y_1 \partial y_2} + \mathrm{i}\frac{\partial^2 H_1}{\partial y_1 \partial y_3}\right),$$

$$g_{011} = \frac{1}{4}\left(\frac{\partial^2 H_1}{\partial y_2^2} + \frac{\partial^2 H_1}{\partial y_3^2}\right),$$

$$G_{100} = \frac{\partial^2 H_1}{\partial y_1 \partial w}, \quad G_{010} = \frac{1}{2}\left(\frac{\partial^2 H_1}{\partial y_2 \partial w} - \mathrm{i}\frac{\partial^2 H_1}{\partial y_3 \partial w}\right),$$

$$G_{001}=\frac{1}{2}\left(\frac{\partial^2 H_1}{\partial y_2\partial w}+\mathrm{i}\,\frac{\partial^2 H_1}{\partial y_3\partial w}\right),\quad g_{300}=\frac{\partial^3 H_1}{\partial y_1^3},\quad g_{111}=\frac{1}{4}\left(\frac{\partial^3 H_1}{\partial y_1\partial y_2^2}+\frac{\partial^3 H_1}{\partial y_1\partial y_3^2}\right),$$

$$h_{200}=\frac{\partial^2 H_2}{\partial y_1^2}+\mathrm{i}\frac{\partial^2 H_3}{\partial y_1^2},\quad h_{020}=\frac{1}{4}\left[\frac{\partial^2 H_2}{\partial y_2^2}-\frac{\partial^2 H_2}{\partial y_3^2}+2\frac{\partial^2 H_3}{\partial y_2\partial y_3}+\mathrm{i}\left(\frac{\partial^2 H_3}{\partial y_2^2}-\frac{\partial^2 H_3}{\partial y_3^2}-2\frac{\partial^2 H_2}{\partial y_2\partial y_3}\right)\right],$$

$$h_{002}=\frac{1}{4}\left[\frac{\partial^2 H_2}{\partial y_2^2}-\frac{\partial^2 H_2}{\partial y_3^2}-2\frac{\partial^2 H_3}{\partial y_2\partial y_3}+\mathrm{i}\left(\frac{\partial^2 H_3}{\partial y_2^2}-\frac{\partial^2 H_3}{\partial y_3^2}+2\frac{\partial^2 H_2}{\partial y_2\partial y_3}\right)\right],$$

$$h_{110}=\frac{1}{2}\left[\frac{\partial^2 H_2}{\partial y_1\partial y_2}+\frac{\partial^2 H_3}{\partial y_1\partial y_3}+\mathrm{i}\left(\frac{\partial^2 H_3}{\partial y_1\partial y_2}-\frac{\partial^2 H_2}{\partial y_1\partial y_3}\right)\right],$$

$$h_{101}=\frac{1}{2}\left[\frac{\partial^2 H_2}{\partial y_1\partial y_2}-\frac{\partial^2 H_3}{\partial y_1\partial y_3}+\mathrm{i}\left(\frac{\partial^2 H_3}{\partial y_1\partial y_2}+\frac{\partial^2 H_2}{\partial y_1\partial y_3}\right)\right],$$

$$h_{011}=\frac{1}{4}\left[\frac{\partial^2 H_2}{\partial y_2^2}+\frac{\partial^2 H_2}{\partial y_3^2}+\mathrm{i}\left(\frac{\partial^2 H_3}{\partial y_2^2}+\frac{\partial^2 H_3}{\partial y_3^2}\right)\right],$$

$$K_{100}=\frac{\partial^2 H_2}{\partial y_1\partial w}+\mathrm{i}\frac{\partial^2 H_3}{\partial y_1\partial w},\quad K_{010}=\frac{1}{2}\left[\frac{\partial^2 H_2}{\partial y_2\partial w}+\frac{\partial^2 H_3}{\partial y_3\partial w}+\mathrm{i}\left(\frac{\partial^2 H_3}{\partial y_2\partial w}-\frac{\partial^2 H_2}{\partial y_3\partial w}\right)\right],$$

$$K_{001}=\frac{1}{2}\left[\frac{\partial^2 H_2}{\partial y_2\partial w}-\frac{\partial^2 H_3}{\partial y_3\partial w}+\mathrm{i}\left(\frac{\partial^2 H_3}{\partial y_2\partial w}+\frac{\partial^2 H_2}{\partial y_3\partial w}\right)\right],$$

$$h_{210}=\frac{1}{2}\left[\frac{\partial^3 H_2}{\partial y_1^2\partial y_2}+\frac{\partial^3 H_3}{\partial y_1^2\partial y_3}+\mathrm{i}\left(\frac{\partial^3 H_3}{\partial y_1^2\partial y_2}-\frac{\partial^3 H_2}{\partial y_1^2\partial y_3}\right)\right],$$

$$h_{021}=\frac{1}{8}\left[\frac{\partial^3 H_3}{\partial y_2^2\partial y_3}+\frac{\partial^3 H_2}{\partial y_2\partial y_3^2}+\mathrm{i}\left(-\frac{\partial^3 H_2}{\partial y_2^2\partial y_3}+\frac{\partial^3 H_3}{\partial y_2\partial y_3^2}\right)\right],$$

$$e_{200}=\frac{\partial^2 E}{\partial y_1^2},\quad e_{020}=\frac{1}{4}\left(\frac{\partial^2 E}{\partial y_2^2}-\frac{\partial^2 E}{\partial y_3^2}-2\mathrm{i}\frac{\partial^2 E}{\partial y_2\partial y_3}\right),$$

$$e_{002}=\frac{1}{4}\left(\frac{\partial^2 E}{\partial y_2^2}-\frac{\partial^2 E}{\partial y_3^2}+2\mathrm{i}\frac{\partial^2 E}{\partial y_2\partial y_3}\right),$$

$$e_{110}=\frac{1}{2}\left(\frac{\partial^2 E}{\partial y_1\partial y_2}-\mathrm{i}\frac{\partial^2 E}{\partial y_1\partial y_3}\right),\quad e_{101}=\frac{1}{2}\left(\frac{\partial^2 E}{\partial y_1\partial y_2}+\mathrm{i}\frac{\partial^2 E}{\partial y_1\partial y_3}\right),$$

$$e_{011}=\frac{1}{4}\left(\frac{\partial^2 E}{\partial y_2^2}+\frac{\partial^2 E}{\partial y_3^2}\right).$$

Suppose now the three-dimensional center manifold has the form

$$w = L(u,z,\bar{z}) = \tfrac{1}{2}W_{200}u^2 + \tfrac{1}{2}W_{020}z^2 + \tfrac{1}{2}W_{002}\bar{z}^2 + W_{110}uz + W_{101}u\bar{z} + W_{011}z\bar{z} + O((|u|+|z|)^3), \tag{38}$$

where $W_{200}, W_{011} \in \mathbf{R}$, and $W_{020} = \bar{W}_{002}$, $W_{110} = \bar{W}_{101}$.

Substituting $w = L(u,z,\bar{z})$ into the first two Eq. (37), we have a three-dimensional reduced map in which f_i $(i = 1,2)$ begin with the third order terms in $(u,z,\bar{z})$, but include no resonant terms of third order.

Due to the properties of center manifold, the equations for $W_{jkl}(j+k+l=2)$ take the following form:

$$[(-1)^j\lambda_0^k\bar{\lambda}_0^l - \lambda_2]W_{jkl} = e_{jkl} \quad (j+k+l=2). \tag{39}$$

It is easy to verify that all matrices $[(-1)^j\lambda_0^k\bar{\lambda}_0^l - \lambda_2]$ are non-singular if $\lambda_0^4 \neq 1$, hence

$$W_{jkl} = [(-1)^j\lambda_0^k\bar{\lambda}_0^l - \lambda_2]^{-1}e_{jkl} \quad (j+k+l=2). \tag{40}$$

The reduced map becomes

$$u' = -u + \sum_{j+k+l=2}\frac{1}{j!k!l!}g_{jkl}u^jz^k\bar{z}^l + \tfrac{1}{6}\hat{g}_{300}u^3 + \hat{g}_{111}uz\bar{z} + \hat{f}_1(u,z,\bar{z}),$$

$$z' = \lambda_0 z + \sum_{j+k+l=2}\frac{1}{j!k!l!}h_{jkl}u^jz^k\bar{z}^l + \tfrac{1}{2}\hat{h}_{210}u^2z + \tfrac{1}{2}\hat{h}_{021}z^2\bar{z} + \hat{f}_2(u,z,\bar{z}), \tag{41}$$

where

$$\begin{aligned}
&\tfrac{1}{6}\hat{g}_{300} = \tfrac{1}{6}g_{300} + \tfrac{1}{2}G_{100}W_{200},\\
&\hat{g}_{111} = g_{111} + G_{100}W_{011} + G_{010}W_{101} + G_{001}W_{110},\\
&\tfrac{1}{2}\hat{h}_{210} = \tfrac{1}{2}h_{210} + K_{100}W_{110} + \tfrac{1}{2}K_{010}W_{200},\\
&\tfrac{1}{2}\hat{h}_{021} = \tfrac{1}{2}h_{021} + K_{010}W_{011} + \tfrac{1}{2}K_{001}W_{020}.
\end{aligned} \tag{42}$$

The next step is to transform (41) into its normal form. We have dropped the "cap" of $\hat{g}_{jkl}$ and $\hat{h}_{jkl}$ $(j+k+l \geqslant 3)$ in Eq. (41). Rewrite Eq. (41) as

$$\begin{aligned}
&\hat{G}: \mathbf{R}\times\mathbf{C} \to \mathbf{R}\times\mathbf{C}, \quad Z' = \hat{G}(Z) = T_0Z + G(Z),\\
&\begin{pmatrix} u' \\ z' \end{pmatrix} = \begin{bmatrix} -1 & 0 \\ 0 & \lambda_0 \end{bmatrix}\begin{pmatrix} x \\ z \end{pmatrix} + \begin{pmatrix} g(x,z,\bar{z}) \\ h(x,z,\bar{z}) \end{pmatrix},
\end{aligned} \tag{43}$$

where

$$Z = \begin{pmatrix} u \\ z \end{pmatrix}, \quad T_0 = \begin{bmatrix} -1 & 0 \\ 0 & \lambda_0 \end{bmatrix}.$$

Suppose

$$G(Z) = G_n(Z) + O(\|Z\|^{n+1}), \tag{44}$$

where G_n is a homogeneous polynomial of degree n ($n \geqslant 2$), i.e.,

$$G_n(Z) = \begin{pmatrix} \sum_{j+k+l=n} \frac{1}{j!k!l!} g_{jkl} u^j z^k \bar{z}^l \\ \sum_{j+k+l=n} \frac{1}{j!k!l!} h_{jkl} u^j z^k \bar{z}^l \end{pmatrix} \quad (n \geqslant 2). \tag{45}$$

In order to cancel the non-resonant terms in Eq. (43), we perform a base change in $\mathbf{R} \times \mathbf{C}$:

$$H : \mathbf{R} \times \mathbf{C} \to \mathbf{R} \times \mathbf{C}, \quad Y = H(Z) = Z + P_n(Z) \tag{46}$$

is a local diffeomorphism in a neighborhood of $(0,0) \in \mathbf{R} \times \mathbf{C}$. P_n has the same form as G_n.Then we have the following diagram:

$$\begin{array}{ccc} \mathbf{R} \times \mathbf{C} & \xrightarrow{\hat{G}} & \mathbf{R} \times \mathbf{C} \\ \downarrow H & & \downarrow H \\ \mathbf{R} \times \mathbf{C} & \xrightarrow{\widehat{N}} & \mathbf{R} \times \mathbf{C} \end{array}$$

and

$$\widehat{N} = H \circ \hat{G} \circ H^{-1}$$

or

$$\begin{aligned} Y' &= \widehat{N}(Y) = T_0 Y + N(Y) \\ &= T_0(Y - P_n(Y) + O(\|Y\|^{n+1})) + G(Y - P_n(Y) + O(\|Y\|^{n+1})) \\ &\quad + P_n(T_0(Y - P_n(Y) + O(\|Y\|^{n+1})) + G(Y - P_n(Y) + O(\|Y\|^{n+1}))) \\ &= T_0 Y + N_n(Y) + O(\|Y\|^{n+1}), \end{aligned} \tag{47}$$

where

$$N_n(Y) = -T_0 P_n(Y) + P_n(T_0 Y) + G_n(Y). \tag{48}$$

The idea of normal form method is to choose $P = P_n$ suitably to kill all non-resonant terms, and leave all resonant ones in G_n unchanged. Let us begin with $n = 2$, and suppose

$$P_2(Z) = \begin{pmatrix} \sum_{j+k+l=2} \frac{1}{j!k!l!} v_{jkl} u^j z^k \bar{z}^l \\ \sum_{j+k+l=2} \frac{1}{j!k!l!} w_{jkl} u^j z^k \bar{z}^l \end{pmatrix},$$

where v_{jkl} and w_{jkl} are unknown constants and are to be determined by equation $N_2(Y) = 0$, that is equivalent to

$$\begin{aligned} &\frac{v_{jkl}}{j!k!l!}[-1 - (-1)^j \lambda_0^k \bar{\lambda}_0^l] = \frac{1}{j!k!l!} g_{jkl} \\ &\qquad\qquad (j + k + l = 2). \\ &\frac{w_{jkl}}{j!k!l!}[\lambda_0 - (-1)^j \lambda_0^k \bar{\lambda}_0^l] = \frac{1}{j!k!l!} h_{jkl} \end{aligned} \tag{49}$$

If $\lambda_0^j \neq 1$ $(j = 1, 3, 4)$, we can choose

$$v_{jkl} = g_{jkl}/[-1 - (-1)^j \lambda_0^k \bar{\lambda}_0^l], \quad w_{jkl} = h_{jkl}/[\lambda_0 - (-1)^j \lambda_0^k \bar{\lambda}_0^l] \tag{50}$$

or

$$v_{200} = -g_{200}/2, \quad v_{020} = -g_{020}/(\lambda_0^2 + 1), \quad v_{002} = -g_{002}/(\bar{\lambda}_0^2 + 1),$$

$$v_{110} = g_{110}/(\lambda_0 - 1), \quad v_{101} = g_{101}/(\bar{\lambda}_0 - 1), \quad v_{011} = -g_{011}/2,$$

$$w_{200} = h_{200}/(\lambda_0 - 1), \quad w_{020} = h_{020}/\lambda_0(1 - \lambda_0), \quad w_{002} = h_{002}/(\lambda_0 - \bar{\lambda}_0^2),$$

$$w_{110} = h_{110}/(2\lambda_0), \quad w_{101} = h_{101}/(\lambda_0 + \bar{\lambda}_0), \quad w_{011} = h_{011}/(\lambda_0 - 1).$$

Now we have moved all second order terms out off Eq. (43). Similar procedure can be applied to $n = 3$: suppose $Y = Z + P_3(Z)$ and obtain the equations similar to Eq. (49), this time, we find that if $\lambda_0^j \neq 1$ $(j = 2, 4, 6)$, all terms in $G_3(Z)$ can be cancelled, but the following terms:

$$\begin{pmatrix} \frac{1}{6} g_{300} u^3 + g_{111} u z \bar{z} \\ \frac{1}{2} h_{210} u^2 z + \frac{1}{2} z^2 \bar{z} \end{pmatrix} \tag{51}$$

cannot be cancelled because the corresponding denominators in Eq. (50) are zero. And we let those terms in P_3 to be zero. So third order base change does not effect the coefficients in Eq. (51). It is easy to verify if adding more conditions on λ_0, i.e., $\lambda_0^4 \neq -1$ and $\lambda_0^5 \neq -1$, we can cancel all fourth order terms in Eq. (43). The fourth order base change does not effect all resonant terms in Eq. (51) either. We at last obtain the following normal form of map (43):

$$\begin{aligned} u' &= -u + a_1 u^3 + a_2 u z \bar{z} + O((|u| + |z|)^5), \\ z' &= \lambda_0 z + b_1 u^2 z + b_2 z^2 \bar{z} + O((|u| + |z|)^5). \end{aligned} \tag{52}$$

Next, we drive the explicit formulae for $a_i, b_i (i = 1, 2)$ in terms of g_{jkl} and h_{jkl} $(j + k + l \leqslant 3)$

Suppose Eq. (46) (for $n = 2$) has inverse

$$Z = Y - P_2(Y) + E_3(Y) + O(\|Y\|^4), \tag{53}$$

where $E_3(Y)$ are homogeneous polynomials of degree 3. And from Eq. (47) (for $n = 2$)

$$\begin{aligned} Y' &= T_0(Y - P_2(Y) + E_3(Y) + O(\|Y\|^4)) \\ &\quad + G(Y - P_2(Y) + E_3(Y) + O(\|Y\|^4)) + P_2(T_0(Y - P_2(Y) + E_3(Y) + O(\|Y\|^4)) \\ &\quad + G(Y - P_2(Y) + E_3(Y) + O(\|Y\|^4))) \\ &= T_0 Y + P_2(T_0 Y) - T_0 P_2(Y) + G_2(Y) + T_0 E_3(Y) + \tilde{G}_2(Y - P_2(Y)) \\ &\quad + \tilde{P}_2(T_0(Y - P_2(Y)) + G_2(Y)) + O(\|Y\|^4), \end{aligned} \tag{54}$$

where $P_2(T_0 Y) - T_0 P_2(Y) + G_2(Y) = 0$ and $\tilde{G}_2(Y - P_2(Y))$, $\tilde{P}_2(T_0(Y - P_2(Y)) + G_2(Y))$ represent third order terms in $G_2(Y - P_2(Y))$ and in $P_2(T_0(Y - P_2(Y)) + G_2(Y))$, respectively. From Eq. (54), we know we need only to determine the coefficients corresponding resonant terms in

$E_3(Y)$. By definition,

$$Y = Z + P_2(Z) = (Y - P_2(Y) + E_3(Y) + O(\|Y\|^4)) + P_2(Y - P_2(Y) + E_3(Y) + O(\|Y\|^4)).$$

It is clearly

$$E_3(Y) = -\tilde{P}_2(Y - P_2(Y)). \tag{55}$$

A direct calculation shows

$$E_3(Y) = \begin{pmatrix} n_{300}u^3 + n_{111}uz\bar{z} + \cdots \\ m_{210}u^2z + m_{021}z^2\bar{z} + \cdots \end{pmatrix},$$

where

$$n_{300} = \tfrac{1}{8}(g_{200})^2 + \mathrm{Re}\left(\frac{g_{110}h_{200}}{(\lambda_0 - 1)^2}\right),$$

$$n_{111} = \tfrac{1}{4}g_{011}(g_{200} - 2\mathrm{Re}(\bar{\lambda}_0 h_{110})) - 2\mathrm{Re}\left(\frac{\lambda_0 g_{020}h_{101}}{(1 + \lambda_0^2)^2}\right) + 2\mathrm{Re}\left(\frac{g_{110}h_{011}}{(\lambda_0 - 1)^2}\right) - 2\frac{\lambda_0 g_{110}g_{101}}{(\lambda_0 - 1)^2},$$

$$m_{210} = \tfrac{1}{2}\frac{h_{200}}{(\lambda_0 - 1)^2}(2g_{110} - \bar{\lambda}_0 h_{020}) + \frac{(h_{110})^2}{4\lambda_0^2} + \frac{h_{101}\bar{h}_{101}}{(\lambda_0 + \bar{\lambda}_0)^2} - \frac{1}{8}\left(\bar{\lambda}_0 h_{110}g_{200} - \frac{4h_{011}\bar{h}_{200}}{(\lambda_0 - 1)(\bar{\lambda}_0 - 1)}\right),$$

$$m_{021} = -\frac{3\bar{\lambda}_0}{2(\lambda_0 - 1)^2}h_{011}h_{020} + \frac{1}{2}\left|\frac{h_{002}}{\lambda_0 - \bar{\lambda}_0^2}\right|^2 + \left|\frac{h_{011}}{\lambda_0 - 1}\right|^2 - \frac{\bar{\lambda}_0}{4}g_{011}h_{110} - \frac{\lambda_0 h_{101}g_{020}}{2(1 + \lambda_0^2)^2}$$

and finally, we have

$$a_1 = \frac{g_{300}}{6} + \frac{g_{200}g_{200}}{4} - \mathrm{Re}\left(\frac{g_{110}h_{200}}{\lambda_0 - 1}\right),$$

$$a_2 = g_{111} + \frac{g_{200}g_{011}}{2} - g_{011}\,\mathrm{Re}(\bar{\lambda}_0 h_{110}) + g_{110}g_{101} - 2\mathrm{Re}\left(\frac{\lambda_0 g_{020}h_{101}}{1 + \lambda_0^2}\right) - 2\mathrm{Re}\left(\frac{g_{110}h_{011}}{\lambda_0 - 1}\right),$$

$$b_1 = \frac{h_{210}}{2} - \frac{h_{200}h_{020}}{2(\lambda_0 - 1)} - \frac{h_{101}\bar{h}_{101}}{\lambda_0 + \bar{\lambda}_0} - \frac{\bar{\lambda}_0 h_{110}h_{110}}{2} - \frac{(\bar{\lambda}_0 + 1)h_{011}\bar{h}_{200}}{2(\bar{\lambda}_0 - 1)^2} - \frac{g_{110}h_{200}}{\lambda_0 - 1} + \frac{h_{110}g_{200}}{4},$$

$$b_2 = \frac{h_{021}}{2} - \frac{(2\lambda_0 - 1)h_{020}h_{011}}{2\lambda_0(\lambda_0 - 1)} - \frac{h_{002}\bar{h}_{002}}{2(\bar{\lambda}_0 - \lambda_0^2)} + \frac{g_{011}h_{110}}{2} + \frac{g_{020}h_{101}}{2(1 + \lambda_0^2)} + \frac{\lambda_0 h_{011}\bar{h}_{011}}{\lambda_0 - 1}.$$

When the control parameters v vary near the neighborhood of (0,0), we can obtain the normal form map with parameters from map (52), which is [11]

$$F_\mu : \mathbf{R} \times \mathbf{C} \to \mathbf{R} \times \mathbf{C},$$
$$\begin{pmatrix} x' \\ z' \end{pmatrix} = \begin{bmatrix} -1 & \\ & \lambda_0 \end{bmatrix} \begin{pmatrix} x \\ z \end{pmatrix} + \begin{pmatrix} -\varepsilon_1 x + a_1 x^3 + a_2 x|z|^2 + O[(|x| + |z|)^5] \\ \lambda_0(\bar{\varepsilon}_2 z + \bar{b}_1 x^2 z + \bar{b}_2 z|z|^2) + O[(|x| + |z|)^5] \end{pmatrix}, \tag{56}$$

where

$$\varepsilon_1 = \varepsilon_1(v) = -\lambda_1(v) - 1 = -\frac{\partial\lambda_1(0,0)}{\partial v_1}v_1 - \frac{\partial\lambda_1(0,0)}{\partial v_2}v_2,$$
$$\bar{\varepsilon}_2 = \bar{\varepsilon}_2(\mu) = \bar{\lambda}_0\lambda_0(v) - 1 = \bar{\lambda}_0\frac{\partial\lambda_0(0,0)}{\partial v_1}v_1 + \bar{\lambda}_0\frac{\partial\lambda_0(0,0)}{\partial v_2}v_2,$$
$$\bar{b}_1 \approx b_1/\lambda_0, \bar{b}_2 \approx b_2/\lambda_0.$$

Let us put Eq. (56) in polar co-ordinates: $z = y\mathrm{e}^{\mathrm{i}\theta}$, then new form of F_μ is

$$F_\mu : \mathbf{R}^2 \times \mathbf{S}^1 \to \mathbf{R}^2 \times \mathbf{S}^1$$

or

$$\begin{pmatrix} x' \\ y' \\ \theta' \end{pmatrix} = \begin{pmatrix} X(x,y,\theta;\mu) \\ Y(x,y,\theta;\mu) \\ \Theta(x,y,\theta;\mu) \end{pmatrix} = \begin{pmatrix} -x - \varepsilon_1 x + a_1 x^3 + a_2 xy^2 + h.o.t. \\ y + \varepsilon_2 y + \beta_1 x^2 y + \beta_2 y^3 + h.o.t. \\ \theta + \arg\lambda_0 + \varepsilon_3 + \gamma_1 x^2 + \gamma_2 y^2 + h.o.t. \end{pmatrix}, \tag{57}$$

where $\varepsilon_2 = |1 + \bar{\varepsilon}_2| - 1$, $\varepsilon_3 = \arg(\bar{\varepsilon}_2)$, $\beta_1 = \mathrm{Re}(\bar{b}_1)$, $\beta_2 = \mathrm{Re}(\bar{b}_2)$, $\gamma_1 = \mathrm{Im}(\bar{b}_1)$, $\gamma_2 = \mathrm{Im}(\bar{b}_2)$.

Because we are interested in curve doubling bifurcation, let us remove the azimuthal term and we obtain the planar map $F_\mu : \mathbf{R}^2 \to \mathbf{R}^2$. Consider F_μ^2 which is the compound of map F_μ and omitting the high order terms, we obtain

$$\begin{pmatrix} X_\mu^2 \\ Y_\mu^2 \end{pmatrix} = \begin{pmatrix} (1 + 2\varepsilon_1)x - 2a_1(1 + 2\varepsilon_1)x^3 - 2a_2(1 + \varepsilon_1 + \varepsilon_2)xy^2 \\ (1 + 2\varepsilon_2)y + 2\beta_1(1 + \varepsilon_1 + \varepsilon_2)x^2 y + 2\beta_2(1 + 2\varepsilon_2)y^3 \end{pmatrix}. \tag{58}$$

We note that map (58) have four fixed points: $(0,0)$, $(0,y)$, $(x,0)$, (x,y), which respectively correspond to trivial fixed point, invariant circle, fixed point of period two, and invariant circles of

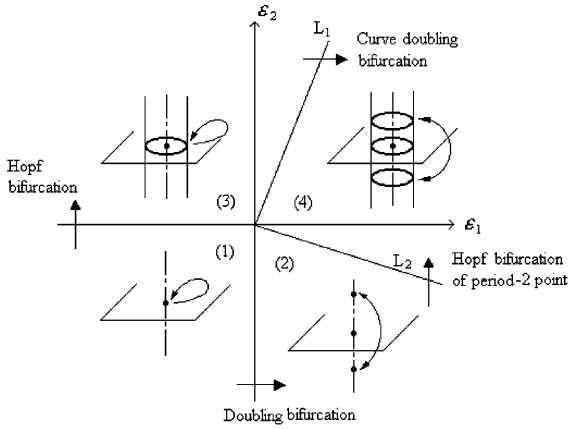

Fig. 2. The normal form unfoldings and phase portrait of Hopf–Flip bifurcation.

order two for three-dimensional map (57) and

(a) invariant circle $(0, y)$: $y = \sqrt{-\varepsilon_2/(\beta_2(1+2\varepsilon_2))}$, for $\varepsilon_2\beta_2 < 0$,
(b) fixed point of period two $(x, 0)$: $x = \pm\sqrt{\varepsilon_1/(a_1(1+2\varepsilon_1))}$, for $\varepsilon_1 a_1 > 0$,
(c) invariant circles of order two (x, y):

$$x = \pm\sqrt{\frac{a_2\varepsilon_2 + \beta_2\varepsilon_1}{A(1+2\varepsilon_1+2\varepsilon_2)}}, \quad y = \sqrt{-\frac{a_1\varepsilon_2 + \beta_1\varepsilon_1}{A(1+2\varepsilon_1+2\varepsilon_2)}},$$

for

$$(a_2\varepsilon_2 + \beta_2\varepsilon_1)/A > 0, \quad (a_1\varepsilon_2 + \beta_1\varepsilon_1)/A < 0 \tag{59}$$

where $A = a_1\beta_2 - a_2\beta_1$.

When $a_1 > 0$, $\beta_2 < 0$, the normal form phase portrait can be easily obtained as shown in Fig. 2. The other possible choices for the signs would give the same kind of result.

In Fig. 2, L_1: $a_2\varepsilon_2 + \beta_2\varepsilon_1 = 0$ or $a_1\varepsilon_2 + \beta_1\varepsilon_1 = 0$; L_2: $a_1\varepsilon_2 + \beta_1\varepsilon_1 = 0$ or $a_2\varepsilon_2 + \beta_2\varepsilon_1 = 0$.

4. Numerical simulations of Hopf–Flip interactions

In this section the analyses developed in the previous section are verified by the presentation of results for the vibro-impact system given in Fig. 1.

We choose the first set of system parameters $\xi = 0.02$, $\beta = 1.891$, $\mu = 0.4$, and take γ and R as the control parameters, $v = (v_1, v_2)^{\mathrm{T}} = (\gamma - \gamma_c, R - R_c)^{\mathrm{T}}$. Acording to the former theoretical analysis and numerical computation, we obtain the critical parameter values γ_c and R_c, the normal form coefficients and eigenvalues of $Df_0(0)$ satisfying conditions (H.1) and (H.2) as follows:

$$\gamma_c = 4.34636, \quad R_c = 0.6053882, \quad \varepsilon_1 = 0.128288v_1 + 6.918943v_2,$$
$$\varepsilon_2 = -0.020036v_1 - 0.101790v_2, \quad \varepsilon_3 = -0.313760v_1 + 0.075331v_2,$$

$$a_1 = 0.183402, \quad a_2 = 0.067188, \quad b_1 = 0.066081 + 0.184888\mathrm{i},$$
$$b_2 = -0.000497 - 0.001383\mathrm{i},$$
$$\beta_1 = 0.196242, \quad \beta_2 = -0.001469, \quad \gamma_1 = -0.006283, \quad \gamma_2 = 0.000050,$$
$$\lambda_1(0) = -1.00000007, \quad \lambda_{2,3}(0) = 0.30625536 \pm 0.95194940\mathrm{i},$$
$$|\lambda_{2,3}(0)| = 1, \quad \lambda_4(0) = -0.345903.$$

The Poincaré section is taken in the form $\sigma = \{(x, \dot{x}, y, \dot{y}, \theta \in \mathbf{R}^4 \times \mathbf{T}, x = y, \dot{x} = \dot{x}_+, y = \dot{y}_+\})$, and the Poincaré map is four dimensional. So the section is projected to the $(y, \dot{y})$ or other planes, which are called projected Poincaré sections. A small perturbation of the theoretical fixed point $X_0 = (\dot{x}_0, x_0, \dot{y}_0, \tau_0)^{\mathrm{T}}$ of periodic 1–1 impact orbit, obtained in Section 2, is taken as an initial point of map in the numerical analyses. As the parameter v vary near the neighborhood of (0,0), dynamic behaviors of the vibro-impact system can be computed by using Eqs. (8)–(10) and impact joint relations (5), which are shown in the projected Poincaré section as Fig. 3. The vibro-impact system exhibits stable periodic 1–1 impact motion (see Fig. 3(a)), corresponding to region (1) in Fig. 2. Fig. 3(b) shows that the vibro-impact system exhibits unstable periodic 1–1 impact motion, corresponding to region (3) in Fig. 2, but in this case invariant circle is not generated. Period

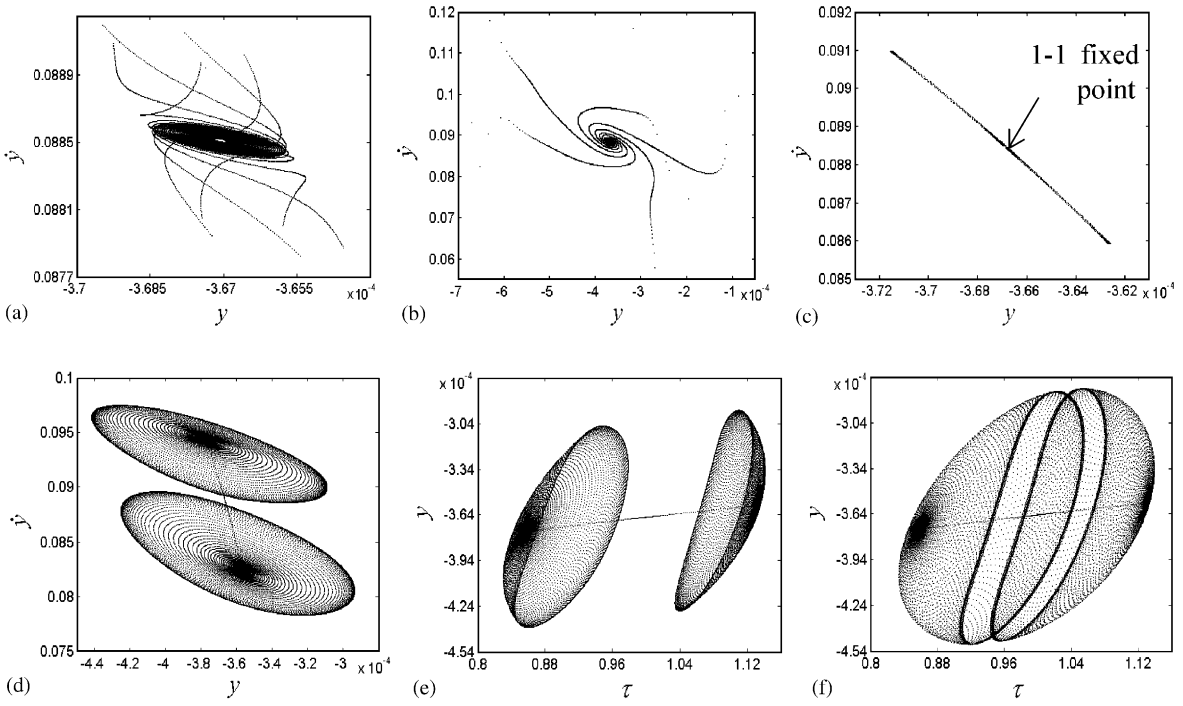

Fig. 3. The projected Poincaré map: (a) $v_1 = 0.002$, $v_2 = -0.0002$, stable 1–1 fixed point; (b) $v_1 = 0.004$, $v_2 = -0.004$, unstable 1–1 fixed point; (c) $v_1 = 0.004$, $v_2 = 0.001$, stable 2–2 fixed points; (d) $v_1 = 0.004$, $v_2 = 0.006$, quasi-periodic impacts represented by the attracting invariant circles from unstable 2–2 fixed points; (e) $v_1 = -0.002$, $v_2 = 0.004$; and (f) $v_1 = -0.01$, $v_2 = 0.004$.

doubling bifurcation of periodic 1–1 impact motion occurs and the system exhibits stable periodic 2–2 impact motion which is represented by two fixed points in projected Poincaré sections as seen in Fig. 3(c), corresponding to region (2) in Fig. 2. The periodic 2–2 impact motion changes its stability as the control parameters vary, and Hopf bifurcation of periodic 2–2 impact motion occurs so that the system can exhibit quasi-periodic impact motion of periodic 2–2 impact points; see Fig. 3(d)–(f), which correspond to region (4) in Fig. 2.

We choose another set of system parameters $\xi = 0.02$, $R = 0.6$, $\mu = 0.7$. γ and β are taken as the control parameters. Let $v = (v_1, v_2)^{\mathrm{T}} = (\gamma - \gamma_c, \beta - \beta_c)^{\mathrm{T}}$, we obtain the critical value of bifurcation parameters, the normal form coefficients and eigenvalues of $Df_0(0)$ satisfying conditions (H.1) and (H.2) as follows:

$$\begin{aligned}
&\gamma_c = 1.6220476, \quad \beta_c = 1.709513, \quad \varepsilon_1 = -9.230864v_1 + 0.054371v_2,\\
&\varepsilon_2 = 1.391321v_1 + 0.415263v_2, \quad \varepsilon_3 = 2.210736v_1 + 0.768962v_2,\\
&a_1 = 0.541371, \quad a_2 = 0.300346, \quad b_1 = 2.391417 - 0.680498\mathrm{i},\\
&b_2 = 0.047815 - 0.673464\mathrm{i},\\
&\beta_1 = -1.329030, \quad \beta_2 = -0.659493,\\
&\gamma_1 = -2.101340, \quad \gamma_2 = 0.144598,\\
&\lambda_1(0) = -1.00000003, \quad \lambda_{2,3}(0) = -0.2828082 \pm 0.9591766\mathrm{i},\\
&|\lambda_{2,3}(0)| = 1, \quad \lambda_4(0) = -0.308326.
\end{aligned}$$

As the parameter v varies near the neighborhood of (0,0), dynamic behaviors of the vibro-impact system are shown in the projected Poincaré section as Fig. 4. The vibro-impact system exhibits stable periodic 1–1 impact motion (see Fig. 4(a)), corresponding to region (1) in Fig. 2. Fig. 4(b) shows that period doubling bifurcation of periodic 1–1 impact motion occurs, but period two fixed points are unstable, corresponding to region (2) in Fig. 2. Hopf bifurcation of 1–1 fixed point occurs and the vibro-impact system exhibits quasi-periodic impacts motion represented by the attracting invariant circle as shown in Fig. 4(c), corresponding to region (3) in Fig. 2. As the control parameters vary, the invariant circle of order one loses stability and curve doubling bifurcation occurs so that the system can exhibit quasi-periodic impact motion represented by two attracting invariant circles as shown in Fig. 4(d) and (e), corresponding to region (4) in Fig. 2.

5. Conclusion

In this paper, we have studied the interaction dynamics of Hopf and period doubling bifurcations of the two-degree-of-freedom vibro-impact system shown in Fig. 1 by theoretical analysis and numerical simulations. Firstly, periodic $n-1$ impact motion and the four-dimensional Poincaré map of the system are established by analytical method and the periodic motion stability is analyzed. When Jacobi matrix of the map has an eigenvalue in -1 and a pair of complex conjugate eigenvalues on the unit circle, the Poincaré map is put into a three-dimensional normal form by using the center manifold theorem and the theory of normal form. In Section 3, we have discussed in detail the local dynamical behavior when the control parameters change near the critical point. Certainly, the method can be extended to other analogous systems. In Section 4,

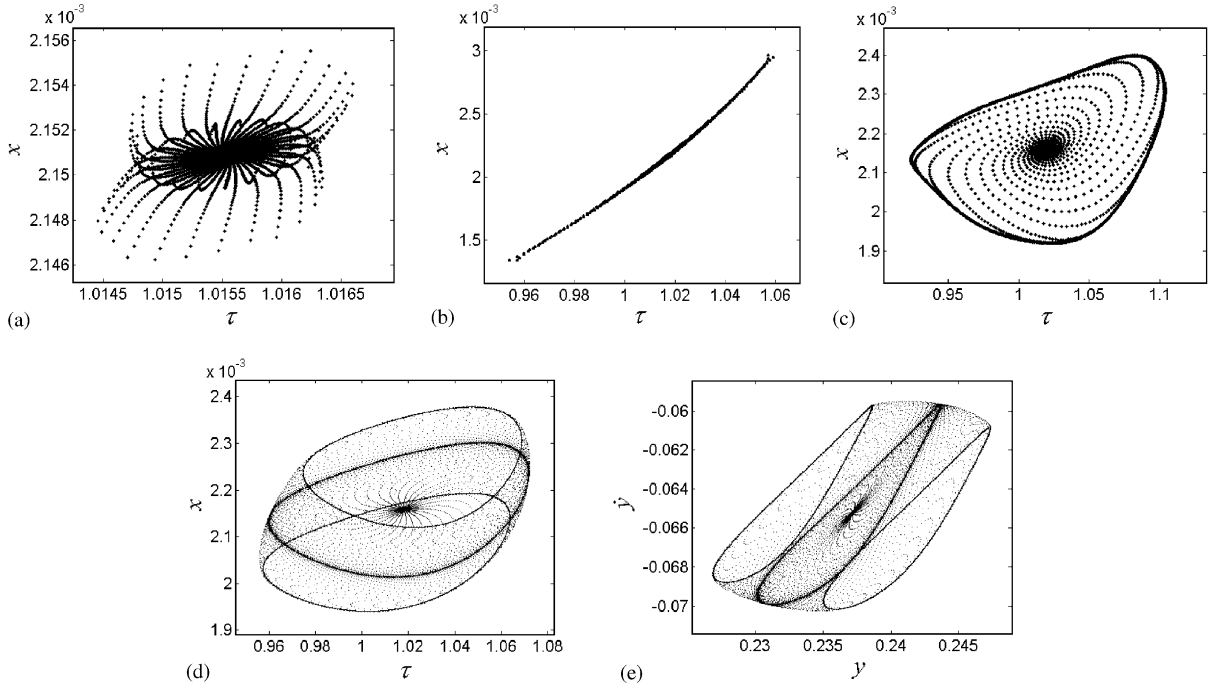

Fig. 4. The projected Poincaré map: (a) $v_1 = 0.0005$, $v_2 = -0.003$, stable 1–1 fixed point; (b) $v_1 = -0.001$, $v_2 = 0.0001$, unstable 2–2 fixed points; (c) $v_1 = 0.0015$, $v_2 = 0.009$, quasi-periodic impacts represented by the attracting invariant circles from unstable 1–1 fixed points; (d, e) $v_1 = 0.0005$, $v_2 = 0.004$, two stable invariant circles via curve doubling bifurcation from unstable invariant circle.

numerical simulations verify the theoretical solution stated and indicate that there exist curve doubling bifurcation (a torus doubling bifurcation), Hopf bifurcation of 2–2 fixed points as well as period doubling bifurcation and Hopf bifurcation of 1–1 fixed points near the critical point.

Acknowledgements

The authors acknowledge the support by National Science Foundation of China (No. 10072051) and the National Education Ministry Foundation of China (20010613001).

Appendix A

$$x_0 = -2\pi\gamma\mu s e_1/\eta[s^2 + (c-1)^2] + \sin\tau_0,$$

$$\dot{x}_0 = (1 - 2\mu R - R)e_1\pi/(1+R),$$

$$\dot{y}_0 = e_1\pi,$$

$$\tau_0 = \cos^{-1}\{e_1\pi[(1 - 2\mu R - R)/(1+R) - 2\mu(\eta(c-1) + \xi s)/\eta(s^2 + (c-1)^2)]\},$$

where

$$s = e^{-2\xi\pi/\gamma}\sin(2\pi\eta/\gamma), \quad c = e^{-2\xi\pi/\gamma}\cos(2\pi\eta/\gamma).$$

Appendix B

$$\frac{\partial f_1}{\partial x} = 1 + \frac{[\eta(c-1)+\xi s](1+R)}{2(1+\mu)\eta},$$

$$\frac{\partial f_1}{\partial \dot{x}} = \frac{(1+R)\gamma s}{2(1+\mu)\eta},$$

$$\frac{\partial f_1}{\partial \dot{y}} = \frac{(1+2\mu-R)\pi}{1+\mu},$$

$$\frac{\partial f_1}{\partial \tau} = \frac{1+R}{2(1+\mu)\eta}[\gamma s\sin\tau_0 + (\eta(c-1)-\xi s)\cos\tau_0],$$

$$\frac{\partial f_2}{\partial x} = -\frac{(1-\mu R)s}{(1+\mu)\eta\gamma} - \frac{[(1-\mu R)a-(1+R)\mu e_1][\eta(c-1)+\xi s](1+R)}{2(1+\mu)^2\eta e_1\pi},$$

$$\frac{\partial f_2}{\partial \dot{x}} = \frac{(1-\mu R)(\eta c-\xi s)\xi}{(1+\mu)\eta} - \frac{[(1-\mu R)a-(1+R)\mu e_1](1+R)\gamma s}{2(1+\mu)^2\eta e_1\pi},$$

$$\frac{\partial f_2}{\partial \dot{y}} = \frac{[(1-\mu R)a+(\mu-R)\mu e_1](1+R)}{(1+\mu)^2 e_1},$$

$$\frac{\partial f_2}{\partial \tau} = \frac{1-\mu R}{(1+\mu)\eta\gamma}[\gamma(\eta(c-1)-\xi s)\sin\tau_0 + s\cos\tau_0] - \frac{[(1-\mu R)a-(1+R)\mu e_1](1+R)}{2(1+\mu)^2\eta e_1\pi}[(\eta(1-c)-\xi s)\cos\tau_0 + \gamma s\sin\tau_0],$$

$$\frac{\partial f_3}{\partial x} = -\frac{(1+R)s}{(1+\mu)\eta\gamma} - \frac{[(1+R)a-(\mu-R)e_1][\eta(c-1)+\xi s](1+R)}{2(1+\mu)^2\eta e_1\pi},$$

$$\frac{\partial f_3}{\partial \dot{x}} = \frac{(1+R)(\eta c-\xi s)\xi}{(1+\mu)\eta} - \frac{[(1+R)a-(\mu-R)e_1](1+R)\gamma s}{2(1+\mu)^2\eta e_1\pi},$$

$$\frac{\partial f_3}{\partial \dot{y}} = -\frac{(1+R)^2 a+(\mu-R)^2 e_1}{(1+\mu)^2 e_1},$$

$$\frac{\partial f_3}{\partial \tau} = \frac{1+R}{(1+\mu)\eta\gamma}[\gamma(\eta(c-1)-\xi s)\sin\tau_0 + s\cos\tau_0] - \frac{[(1+R)a-(\mu-R)e_1](1+R)}{2(1+\mu)^2\eta e_1\pi}[(\eta(1-c)-\xi s)\cos\tau_0 + \gamma s\sin\tau_0],$$

$$\frac{\partial f_4}{\partial x} = -\frac{[\eta(c-1)+\xi s](1+R)}{2(1+\mu)\eta e_1 \pi},$$

$$\frac{\partial f_4}{\partial \dot{x}} = -\frac{(1+R)\gamma s}{2(1+\mu)\eta e_1 \pi},$$

$$\frac{\partial f_4}{\partial \dot{y}} = \frac{1+R}{(1+\mu)e_1},$$

$$\frac{\partial f_4}{\partial \tau} = 1 - \frac{1+R}{2(1+\mu)\eta e_1 \pi}[(\eta(1-c)-\xi s)\cos\tau_0 + \gamma s \sin\tau_0],$$

where

$$a = \ddot{x}(2\pi^-) = -\frac{1}{\gamma}\left\{\frac{2(1+2\mu-R)\xi e_1 \pi}{(1+R)} - \frac{2\pi\mu s e_1}{[s^2+(c-1)^2]\eta} + \gamma \sin\tau_0 - 2\xi\cos\tau_0\right\}.$$

References

[1] S.W. Shaw, P.J. Holmes, A periodically forced piece wise linear oscillator, *Journal of Sound and Vibration* 90 (1983) 129–155.

[2] A.B. Nordmark, Non-periodic motion caused by grazing incidence in an impact oscillator, *Journal of Sound and Vibration* 145 (1991) 279–297.

[3] F. Peterka, J. Vcacik, Transition to chaotic motion in mechanical systems with impacts, *Journal of Sound and Vibration* 154 (1992) 95–115.

[4] S. Chatterjee, A.K. Mallik, Bifurcations and chaos in autonomous self-excited oscillators with impact damping, *Journal of Sound and Vibration* 191 (1996) 539–562.

[5] C. Budd, F. Dux, A. Cliffe, The effect of frequency and clearance variations on single-degree-of-freedom impact oscillators, *Journal of Sound and Vibration* 184 (1995) 475–502.

[6] G.W. Luo, J.H. Xie, Bifurcations and chaos in a system with impacts, *Physica D* 148 (2001) 183–200.

[7] G.W. Luo, J.H. Xie, Hopf bifurcation of a two-degree-of-freedom vibro-impact system, *Journal of Sound and Vibration* 213 (1998) 391–408.

[8] G.W. Luo, J.H. Xie, X.F. Sun, Quasi-periodic and chaotic behaviour of a two-dergree-of-freedom impact in a strong resonance case, *Acta Mechanica Solida Sinica* 12 (1999) 279–283.

[9] J.H. Xie, Codimension two bifurcations and Hopf bifurcations of an impacting vibrating system, *Applied Mathematics and Mechanics* 17 (1996) 65–75.

[10] G.L. Wen, Codimension-2 Hopf bifurcation of a two-degree-of-freedom vibro-impact system, *Journal of Sound and Vibration* 242 (2001) 475–485.

[11] G. Iooss, J.E. Los, Quasi-genericity of bifurcations to high dimensional invariant tori for maps, *Communications in Mathematical Physics* 119 (1988) 453–500.

[12] A.K. Yuri, *Elements of Applied Bifurcation Theory*, Springer, Berlin, 1998.

[13] J.H. Xie, G.L. Wen, J. Xiao, Determining bifurcation parameters of two-degree-of-freedom vibro-impact system, *Journal of Vibration Engineering* 14 (2001) 285–290.